(2) Ouhadi, T.; Fayt, R.; Jerome, R.; Teyssie, Ph. *J. Polym. Sci: Part B: Polym. Phys.* **1986**, *24*, 973.
(3) Paul, D. R. In *Thermoplastic Elastomers*; Legge, N. R., Holden, G., Schroeder, H. E., Eds.; Hanser Publishers: New York, 1987; Chapter 12, Section 6, p 431.
(4) Riess, G. In *Thermoplastic Elastomers*; Legge, N. R., Holden, G., Schoreder, H. E., Eds.; Hanser Publishers: New York, 1987, Chapter 12, Section 2, p 325.
(5) Eastmond, G. C. In *Polymer Surfaces and Interfaces*; Feast, W. J., Munro, H. S., Eds.; Wiley: New York, 1987; p 119.
(6) Edwards, S. F. *Proc. Phys. Soc. London* **1965**, *85*, 613. Freed, K. F. *Adv. Chem. Phys.* **1972**, *22*, 1. Helfand, E. H. *J. Chem. Phys.* **1975**, *62*, 999. Hong, K. M.; Noolandi, J. *Macromolecules* **1981**, *14*, 727.
(7) Noolandi, J.; Hong, K. M. *Macromolecules* **1982**, *15*, 482.
(8) Noolandi, J.; Hong, K. M. *Macromolecules* **1984**, *17*, 1531.
(9) Vilgis, T. A.; Noolandi, J. *Makromol. Chem., Macromol. Symp.* **1988**, *16*, 225.
(10) Noolandi, J.; Kavassalis, T. A. In *Molecular Conformation and Dynamics of Macromolecules in Condensed Systems, Studies in Polymer Science*; Nagasawa, M., Ed.; Elsevier Science Publishers: Amsterdam, The Netherlands, 1988; Vol. 2, p 285.
(11) Meier, D. J. In *Thermoplastic Elastomers*; Legge, N. R., Holden, G., Schroeder, H. E., Eds.; Hanser Publishers: New York, 1987; Chapter 11, p 269.
(12) Brown, R. A.; Masters, A. J.; Price, C.; Yuan, X. F. In *Comprehensive Polymer Science*; Pergamon Press: New York, 1989; Vol. 2, p 155.
(13) Paul, D. R.; Barlow, J. W. *Polymer* **1984**, *25*, 487.
(14) Whitmore, M. D.; Noolandi, J. *Macromolecules* **1985**, *18*, 657.

Effects of Long-Range Polymer–Pore Interactions on the Partitioning of Linear Polymers

Nelson P. Lin and William M. Deen*

Department of Chemical Engineering, 66-509, Massachusetts Institute of Technology, Cambridge, Massachusetts 02139

Received June 13, 1989; Revised Manuscript Received December 15, 1989

ABSTRACT: A "diffusion–reaction" equation is used to describe the effects of long-range polymer–pore interactions on equilibrium partition coefficients for linear polymers between dilute bulk solution and cylindrical or slit-like pores. Results are presented for square-well potentials, electrostatic double-layer potentials, and van der Waals potentials. Intramolecular potentials were neglected in these calculations. In general, a weak potential acting over a large fraction of the pore cross section was found to have a greater effect on partitioning than a stronger but shorter ranged potential. In other words, the partition coefficient did not correlate very well with the average potential, a result of steric exclusion of polymer chains by the pore wall. For attractive polymer–pore interactions, conditions are identified which correspond to a transition from free to weakly adsorbed polymer.

Introduction

The partitioning of macromolecular solutes between small pores and bulk solution underlies various chromatographic and membrane separation processes and is important also in heterogeneous catalysis. This phenomenon is characterized by the partition coefficient, Φ, which is the pore-to-bulk concentration ratio at equilibrium. For rigid solutes, the theoretical results available for Φ encompass "neutral" molecules having a wide variety of shapes and pore geometries ranging from cylinders to the interstices in an array of randomly oriented fibers.[1-3] Whereas the studies just cited focus on purely steric exclusion for very dilute solutions, additional results are available for other solute–pore potentials[4,5] and/or for finite solute concentration,[6-9] in the case of rigid, spherical molecules.

Fewer quantitative predictions of Φ are available for flexible macromolecules, such as long-chain linear polymers. Casassa[10] and Casassa and Tagami[11] exploited the well-known analogy between the random motion of a Brownian particle and the conformation of a freely jointed polymer chain. This enabled them to calculate Φ for neutral polymers (linear or star shaped) by solving an analogue to a transient diffusion equation. For a chain consisting of N mass points connected by rectilinear segments of length l, this continuum approach requires that N be very large and that l be much smaller than the characteristic pore dimension (e.g., the pore radius r_p). Davidson et al.[12] used Monte Carlo simulations to calculate Φ for freely jointed chains, enabling them to obtain results for moderate values of N and l/r_p.

Theoretical results for linear polymers with long-range polymer–pore interactions are even more limited. Davidson et al.[12] reported a few values of Φ from Monte Carlo simulations which included attractive potentials, and Davidson and Deen[13] have recently performed the analogous continuum, "diffusion equation" calculation. Both studies considered only attractive potentials of a particular form, a square well of width comparable to the segment length, l. Zhulina et al.[14] and Gorbunov et al.[15] used lattice models to examine the effects of polymer–pore interactions on the partitioning of long chains in slit-like pores and pores of square cross section, respectively. Pouchlý[16] used the diffusion equation approach to describe partitioning in pores with permeable walls, including surface forces near the walls.

The objective of the present study was to estimate Φ for long chains experiencing various attractive or repulsive polymer–pore potentials. To do this, we have extended the diffusion equation method of Casassa to account for long-range interactions. Our approach was to add a source or sink term to the diffusion equation, as has been done in modeling the excluded volume of linear polymers[17,18]

0024-9297/90/2223-2947$02.50/0 © 1990 American Chemical Society

and the adsorption of polymers on planar surfaces.[19-21] We have found this to be a very efficient method to calculate Φ for various assumed potentials, in pores having regular shapes.

We begin by formulating the partitioning problem in terms of configuration integrals and then discuss how these integrals may be evaluated from the solution of a "diffusion–reaction" equation with suitable initial and boundary conditions. This initial development is more explicit and more general than that published previously for random coil polymers[10,13] and allows previous partitioning calculations to emerge as special cases. Results are presented for attractive or repulsive square-well potentials, for electrostatic double-layer potentials, and for van der Waals potentials, in cylindrical or slit-like pores.

Model Formulation

Partition Coefficient and Configuration Integrals. The partition coefficient for a dilute solution can be calculated as the ratio of configuration integrals for the macromolecular solute in the pore and in bulk solution:[1]

$$\Phi = \frac{\int\int\int \mathrm{d}\mathbf{r}\,\mathrm{d}\Omega\,\mathrm{d}\Gamma\, e^{-E^*/kT}}{\int\int\int \mathrm{d}\mathbf{r}\,\mathrm{d}\Omega\,\mathrm{d}\Gamma\, e^{-E/kT}} \tag{1}$$

where $\mathbf{r}$, Ω, and Γ are coordinate vectors describing, respectively, solute position, orientation, and conformation. E^* and E are the configuration energies for the pore and bulk solution, k is Boltzmann's constant, and T is absolute temperature. The position, $\mathbf{r}$, is defined as the position of some arbitrary locator point on the solute. For rigid solutes, this locator point is usually taken to be the center of mass.

The configuration energies can be expressed as

$$E^* = E_{\mathrm{MP}}(\mathbf{r},\Omega,\Gamma) + E_{\mathrm{M}}(\Gamma) + E_{\mathrm{MS}}(\Gamma) \tag{2a}$$

$$E = E_{\mathrm{M}}(\Gamma) + E_{\mathrm{MS}}(\Gamma) \tag{2b}$$

where E_{MP} is the energy associated with solute–pore interactions, E_{M} is the energy due to intramolecular forces, and E_{MS} is the contribution of solute–solvent interactions. The bulk configuration energy, E, is a function of conformation only, because the energy of a solute in bulk solution is independent of position and orientation. By use of the energies defined in eq 2, eq 1 can be rewritten:

$$\Phi = \frac{\int\int\int \mathrm{d}\mathbf{r}\,\mathrm{d}\Omega\,\mathrm{d}\Gamma\, e^{-[E_{\mathrm{MP}}(\mathbf{r},\Omega,\Gamma)+E_{\mathrm{M}}(\Gamma)+E_{\mathrm{MS}}(\Gamma)]/kT}}{\int\int\int \mathrm{d}\mathbf{r}\,\mathrm{d}\Omega\,\mathrm{d}\Gamma\, e^{-[E_{\mathrm{M}}(\Gamma)+E_{\mathrm{MS}}(\Gamma)]/kT}} \tag{3}$$

As a specific example of the use of eq 3, consider the case of a spherical solute of radius λ and an infinitely long cylindrical pore of unit radius. Because the solute is rigid, there is only one possible conformation, and no integration over Γ is necessary. Therefore, the terms involving E_{M} and E_{MS} in the numerator and denominator of eq 3 will cancel. In addition, because of the symmetry of the sphere, all orientations are equivalent. The partition coefficient is simply

$$\Phi = \frac{\int_0^{1-\lambda} r\,\mathrm{d}r\, e^{-E_{\mathrm{MP}}(r)/kT}}{\int_0^1 r\,\mathrm{d}r} \tag{4}$$

where r is the radial position of the center of the sphere. This is the expression used by Smith and Deen[4] in calculating the partition coefficient for a charged sphere in a charged, cylindrical pore. The upper limit of integration in the numerator arises from steric exclusion (i.e., $E_{\mathrm{MP}} = \infty$ for $r > 1 - \lambda$).

As a first approximation to the effects of long-range solute–pore interactions on the partitioning of linear polymers, we will assume that the terms involving E_{M} and E_{MS} cancel one another. For uncharged polymers, this is equivalent to assuming that Θ conditions prevail. For polyelectrolytes, it implies that the intramolecular electrostatic repulsions which contribute to E_{M} are weak and therefore not strongly dependent on Γ. An equivalent assumption was employed by Wiegel[21] in modeling adsorption of polyelectrolytes. With these assumptions, eq 3 becomes

$$\Phi = \frac{\int\int\int \mathrm{d}\mathbf{r}\,\mathrm{d}\Omega\,\mathrm{d}\Gamma\, \exp[-E_{\mathrm{MP}}(\mathbf{r},\Omega,\Gamma)/kT]}{\int\int\int \mathrm{d}\mathbf{r}\,\mathrm{d}\Omega\,\mathrm{d}\Gamma} \tag{5}$$

Diffusion–Reaction Equation. We will model linear polymers as chains consisting of N mass points connected by $N - 1$ segments, each of length l. For a random coil, the probability of finding mass point $j + 1$ at position $\mathbf{R}$, $P(\mathbf{R},j+1)$, is governed by a Markoff integral equation[18]

$$P(\mathbf{R},j+1) = \int P(\mathbf{R}-\mathbf{r},j)\Upsilon(\mathbf{r})e^{-\phi(\mathbf{R})}\,\mathrm{d}\mathbf{r} \tag{6}$$

In eq 6, $\mathbf{r}$ is the vector from mass point j to mass point $j + 1$, Υ is the effective bond probability, and $\phi(\mathbf{R})$ is the dimensionless energy associated with a mass point located at $\mathbf{R}$. For a given molecular configuration in a pore, assuming additive segment–pore energies

$$\frac{E^*}{kT} = \sum_{i=1}^{N} \phi_i \tag{7}$$

where ϕ_i is the energy of the ith mass point. However, as described below, it is not necessary to calculate ϕ_i for each mass point and configuration.

For fixed segment length l

$$\Upsilon(\mathbf{r}) = \frac{\delta(|\mathbf{r}| - l)}{4\pi l^2} \tag{8}$$

where δ is the Dirac δ function. For $j \gg 1$, eq 6 can be integrated to obtain[13]

$$\frac{\partial P(\mathbf{R},j)}{\partial j} = \frac{e^{-\phi(\mathbf{R})}l^2\nabla^2 P(\mathbf{R},j)}{6} + [e^{-\phi(\mathbf{R})} - 1]P(\mathbf{R},j) \tag{9}$$

For $\phi(\mathbf{R}) \ll 1$, we obtain the "diffusion–reaction" equation employed here:

$$\frac{\partial P}{\partial J} = \frac{Nl^2}{6}\nabla^2 P - N\phi(\mathbf{R})P \tag{10}$$

where $J = j/N$ and $0 \le J \le 1$ for large N. Equation 10 is of course analogous to the conservation equation describing transient diffusion with a first-order homogeneous reaction. The "diffusion coefficient" is $Nl^2/6 = r_g^2$, where r_g is the root-mean-square radius of gyration for a random coil in bulk solution.[22] The potential term $N\phi$ is analogous to a first-order rate constant, whereas J takes the place of time. A derivation of eq 10 given by de Gennes[23] begins with a lattice model, so that the integral in eq 6 is replaced by a summation over adjacent lattice sites. Because the assumption $\phi \ll 1$ is introduced early in that derivation, eq 9 is not obtained as an intermediate step. With $N\phi = 0$, eq 10 is equivalent to the diffusion equation employed by Casassa.[10] Note that P is not a normalized probability; $P(\mathbf{R},j)$ is a relative mea-

sure of the number of ways that the jth mass point can occupy position **R**.

Application of Diffusion–Reaction Equation. We now describe how eq 10 can be used to calculate the partition coefficient for a random coil in a long cylindrical pore, provided that $l/r_p \ll 1$ (r_p is the pore radius). Because the permissibility of a chain configuration depends only on the radial position of each mass point of the chain and because ϕ is assumed to depend only on r, we can write eq 10 in cylindrical coordinates without regard to angular or axial position:

$$\frac{\partial P}{\partial J} = \lambda_g^2\left(\frac{\partial^2 P}{\partial r^2} + \frac{1}{r}\frac{\partial P}{\partial r}\right) - N\phi(r)P \tag{11}$$

where r is radial position normalized by r_p ($0 \le r \le 1$) and $\lambda_g = r_g/r_p$. DiMarzio[24] showed that the "absorbing wall" boundary condition

$$P(1,J) = 0 \tag{12}$$

correctly excludes all chain configurations which would penetrate the pore wall. The symmetry of the pore provides the other boundary condition:

$$\frac{\partial P}{\partial r}(0,J) = 0 \tag{13}$$

As discussed by Casassa,[10] $P(r,J)$ now measures the probability of finding the jth mass point at position r in the pore, given that no preceding mass point overlaps with the wall.

The final key to using $P(r,J)$ to calculate Φ is the initial condition employed with eq 11. First, consider an instantaneous point source: $P(r',0) = 1$. This condition fixes the first mass point of the chain at position r' and yields a solution denoted by $P(r,J|r')$. $P(r,1|r')$ then measures the number of ways in which mass point N can occupy position r, given that the first mass point is fixed at r' and that no part of the chain overlaps the wall. If we now integrate $P(r,1|r')$ over r, we obtain the fraction of all chains emanating from position r' which will fit inside the pore. In terms of the formalism of eq 1, we have chosen the first mass point of the chain to be the locator point for the macromolecule. By integrating $P(r,1|r')$ over all r, we have accounted for all possible chain configurations with position r'; in other words, we have allowed the chain to sample all conformations and orientations. It follows that

$$\int_0^1 P(r,1|r')r\,dr = \int\int d\Omega\,d\Gamma\,\exp[-E_{MP}(r',\Omega,\Gamma)/kT] \tag{14}$$

Thus, the numerator of eq 5 could be calculated by integrating the left-hand side of eq 14 over all r' ($0 \le r' \le 1$). A similar calculation, but with $E_{MP} = 0$, would yield the denominator, thereby permitting evaluation of Φ.

A much more convenient approach, however, is to use an initial condition which has the effect of beginning chains simultaneously at all radial positions.[10] With long-range interactions, this condition is

$$P(r,0) = e^{-\phi(r)} \quad \text{for all } r \tag{15}$$

If the solution to eq 11 with initial condition eq 15 is denoted by $P(r,J)$, then $P(r',1)$ measures the number of ways the Nth mass point can be found at position r', given that the "beginning" of the chain is free to sample all positions in the pore. This situation is basically the same as that described by eq 14, except for which chain end is considered fixed. In other words, the locator point in one case is mass point 1 and in the other case mass point N. However, because the two ends of the chain are indistinguishable, the two situations are identical. Thus

$$P(r',1) = \int_0^1 P(r,1|r')r\,dr \tag{16}$$

Finally, the partition coefficient can be calculated:

$$\Phi = \frac{\int_0^1 P(r,1)r\,dr}{\int_0^1 r\,dr} \tag{17}$$

Thus, point-source solutions are not needed to evaluate Φ. The extension of this approach to other regular pore geometries is straightforward.

In obtaining eqs 10 and 11 from eq 9, it was assumed that $\phi \ll 1$. In this case, eq 15 reduces to

$$P(r,0) = 1 \quad \text{for all } r \tag{18}$$

We therefore used eq 18 as the initial condition for eq 11. This initial condition is identical with that employed by Casassa[10] for neutral polymers ($\phi = 0$). It was also used by Davidson and Deen[13] for calculations where ϕ was not small. In that case, however, ϕ was nonzero only in a layer of vanishing width next to the pore wall, so eq 18 was valid asymptotically. Although not stated or employed previously, eq 15 is in general the correct initial condition to use with eq 9. This point is illustrated in the Appendix, by use of a "discrete" example involving a chain of two segments.

Potential Energy Functions. Square-Well Potential. As a simple approximation to polymer–pore interactions, we considered a square-well potential extending a dimensionless distance d (relative to r_p) from the pore wall. The energy term in eq 11 then takes the form

$$N\phi(r) = 0 \quad 0 \le r < 1 - d$$
$$N\phi(r) = W \quad 1 - d < r \le 1 \tag{19}$$

With this form of the potential, eq 11 with boundary conditions eqs 12 and 13 and initial condition eq 18 can be solved analytically. The solutions for both cylindrical and slit-like pores are outlined in the Appendix. For the cylindrical pore, we integrated eq 17 using Simpson's rule to obtain the partition coefficient. A similar calculation using Cartesian coordinates yielded results for slit (parallel-plane) pores.

Electrostatic Potential. For a linear polymer of total charge $\hat{q}$, we approximated the electrostatic interaction energy by neglecting intramolecular forces. With this assumption, each mass point of the polymer chain experiences an energy as if it were alone in a charged pore. This energy is the product of the charge on the mass point ($\hat{q}/N$) and the electrostatic potential in the pore ($\hat{\psi}$)

$$\phi(r) = \frac{\hat{q}\hat{\psi}}{NkT} \tag{20}$$

The electrostatic potential within a charged pore can be estimated from the linearized Poisson–Boltzmann equation:

$$\nabla^2\hat{\psi} = \kappa^2\hat{\psi} \tag{21}$$

where κ is the inverse Debye length. For a pore of surface charge density $\hat{\sigma}$ through a medium of low dielectric constant, the appropriate boundary conditions are[4]

$$\left.\frac{d\hat{\psi}}{d\hat{r}}\right|_{r_p} = \frac{\hat{\sigma}}{\epsilon} \tag{22}$$

$$\left.\frac{d\hat{\psi}}{d\hat{r}}\right|_0 = 0 \tag{23}$$

where $\hat{r}$ is the radial coordinate and ϵ is the dieletric permittivity of the solvent. If the pore radius, r_p, is chosen as the reference length, the dimensionless radial coordinate and inverse Debye length become

$$r = \hat{r}/r_p \tag{24}$$

$$\tau = \kappa r_p \tag{25}$$

We define the dimensionless molecular charge, pore-wall charge density, and electrostatic potential as, respectively

$$q = \frac{\hat{q}e}{\epsilon kTr_p} \tag{26}$$

$$\sigma = \frac{\hat{\sigma}er_p}{\epsilon kT} \tag{27}$$

$$\psi = \frac{\hat{\psi}e}{kT} \tag{28}$$

where e is the elementary charge. In these dimensionless variables, the solution for the electrostatic potential is

$$\psi = \frac{\sigma I_0(\tau r)}{\tau I_1(\tau)} \tag{29}$$

where I_0 and I_1 are modified Bessel functions of the first kind of order zero and one, respectively. The potential required for eq 11 is now

$$N\phi(r) = \frac{\xi q\sigma I_0(\tau r)}{\tau I_1(\tau)} \tag{30}$$

where

$$\xi = \frac{\epsilon kTr_p}{e^2} \tag{31}$$

For slit pores, the resulting energy is

$$N\phi(y) = \frac{\xi q\sigma \cosh(\tau y)}{\tau \sinh(\tau)} \tag{32}$$

where y is zero at the pore center and one at the pore wall and r_p is replaced by the slit half-width. With the potential defined by either eq 30 or 32, we obtained $P(\mathbf{R},\mathcal{J})$ by using the Crank–Nicholson algorithm[25] to integrate eq 10.

van der Waals Potential. To obtain a van der Waals interaction energy, we again considered only the interaction between one mass point of the polymer chain and the pore wall. We approximated the potential as a power-law attraction combined with a hard-sphere repulsion. For the energy of one mass point located a dimensionless distance x from a differential volume element of the pore wall dV, we have

$$N\,d\phi(x) = \infty \qquad x < s$$

$$N\,d\phi(x) = \frac{-cn}{x^6}dV \qquad x > s \tag{33}$$

where s is the dimensionless hard-sphere radius, c represents the energy per molecule (relative to kT), and n is the number density of molecules in the pore wall. We obtained the total van der Waals energy by integrating eq 33 over the volume of the wall. In so doing, we assumed additivity of the van der Waals forces. For a particle between two semi-infinite plane walls

$$N\phi(y) = \infty \qquad 1 - s < y < 1$$

$$N\phi(y) = -C\left[\frac{1}{(1-y)^3} + \frac{1}{(1+y)^3}\right] \qquad 0 \le y \le 1 - s \tag{34}$$

where $C = \pi cn/6$ and y is the dimensionless distance from the mid-plane. As with the electrostatic interaction, we numerically integrated eq 10 using the Crank–Nicholson algorithm. Although the van der Waals energy in a cylindrical pore can be derived in an analogous fashion, the calculation requires numerical integration in two dimensions. We obtained van der Waals results only for slit pores.

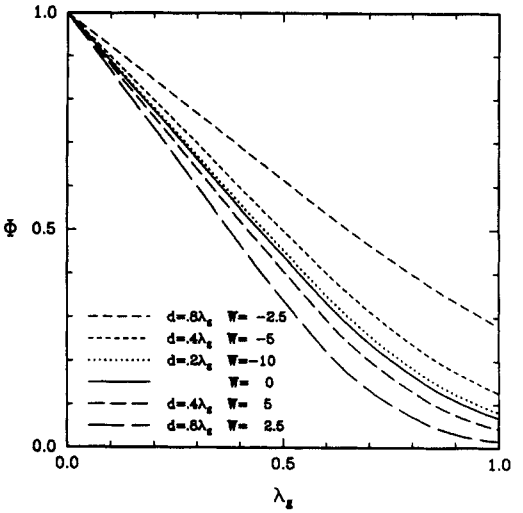

Figure 1. Partition coefficient as a function of solute-to-pore size ratio for square-well potentials of width d and depth W in a slit pore. In this case, λ_g is the radius of gyration divided by the pore half-width.

Results

The results are presented as plots of the partition coefficient (Φ) versus the molecular-to-pore size ratio (λ_g), for various assumed potentials. Figure 1 shows results for both attractive and repulsive square-well potentials in slit pores. The parameter d was varied in proportion to λ_g, so the square-well width was a constant fraction of r_g. For comparative purposes, the integral of the potential over position was held constant for the three attractive wells ($W < 0$) and for the two repulsive wells ($W > 0$). Whether the interaction is attractive or repulsive, a weak potential acting over a large fraction of the pore is seen to have a greater effect on partitioning than does a stronger but shorter ranged potential. In the limit as $d \to 0$, the results approach those for neutral polymers ($W = 0$), regardless of the value of W. The results for cylindrical pores are qualitatively similar to those shown in Figure 1. For the same parameter values, Φ for cylindrical pores is lower than for slits, at any given value of λ_g.

Figure 2 shows results for electrostatic interactions in cylindrical pores, for various values of the polymer–pore charge product, $q\sigma$. Molecular size (r_g) was fixed throughout, λ_g varying as a result of changes in pore radius only. The Debye length was also taken to be constant. Accordingly, the quantities $\tau\lambda_g$ and $\xi\lambda_g$ were held fixed. As expected, Φ decreased for polymer and pore charges of like sign and increased for polymer and pore charges of opposite sign, relative to an uncharged system with the same value of λ_g. The results for attractive interactions ($q\sigma < 0$) represent competing effects of entropy and

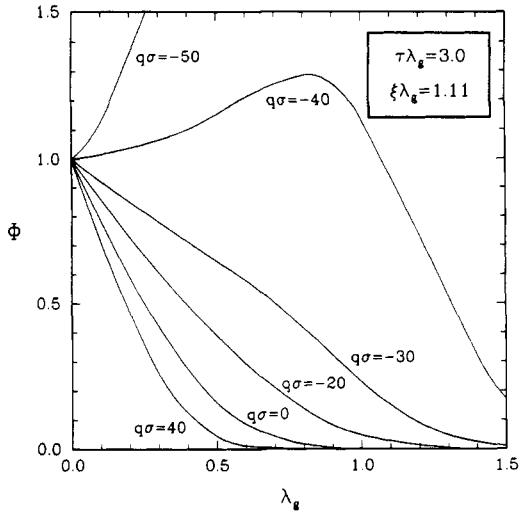

Figure 2. Partition coefficient for electrostatic potentials in a cylindrical pore, for various values of the product of polymer and pore charge ($q\sigma$). Radius of gyration and Debye length are held constant, so that $\tau\lambda_g$ and $\xi\lambda_g$ are constant throughout.

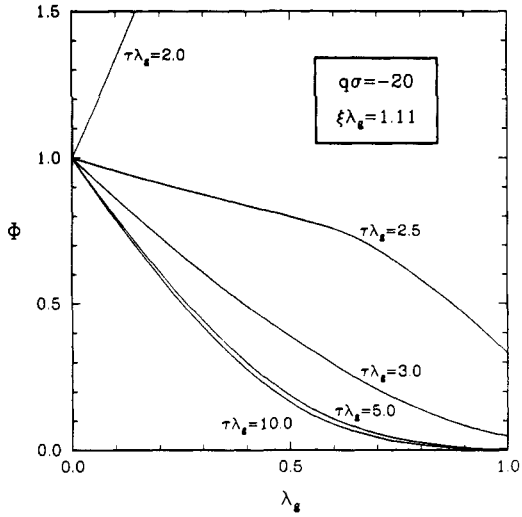

Figure 3. Partition coefficient for electrostatic potentials in a cylindrical pore, for various values of Debye length. As in Figure 2, r_g is held constant.

enthalpy, as illustrated most clearly for $q\sigma = -40$. For this combination of charges, the favorable enthalpy difference between pore and bulk solution predominates for small λ_g, and therefore $\Phi > 1$. However, as λ_g increases, the entropic restrictions in the pore become increasingly important, and eventually $\Phi \to 0$ for large λ_g. As a result, the maximum Φ is at an intermediate size ratio, $\lambda_g \simeq 0.85$ for $q\sigma = -40$. Although not shown on the scale of Figure 2, Φ for $q\sigma = -50$ also reaches a maximum at intermediate λ_g and eventually decays to zero as λ_g is increased further. The value of $q\sigma$ for which $\Phi = 1$ (at a given λ_g) is analogous to the critical energy for adsorption of a polymer on a planar surface.[17,19-21] This analogy and the prediction of the critical energy are discussed in detail in the Appendix. Thus, the results in this and subsequent figures (where $\Phi > 1$) may be interpreted as representing polymer adsorption, although the calculation of Φ makes no distinction between free and bound polymer.

Results for electrostatic interactions at a fixed charge ($q\sigma = -20$) but with varying Debye length are shown in Figure 3. As before, molecular size has been held constant. As $\tau\lambda_g$ is increased (Debye length decreased), the charge interactions are increasingly screened, and the neutral limit is eventually reached. The curve for $\tau\lambda_g = 10$ is indistinguishable from that for an uncharged macromolecule and pore. Large values of $\tau\lambda_g$ have the same effect as small values of d/λ_g for the square-well potential: in both instances, the interaction is too short ranged to be important. It is evident also that there is a critical value of $\tau\lambda_g$ at which $\Phi = 1$ (for fixed $q\sigma < 0$), just as there is a critical value of $q\sigma$.

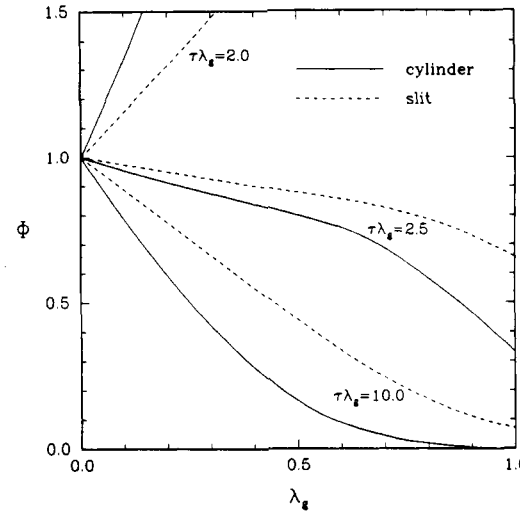

Figure 4. Comparison of partition coefficient for cylindrical and slit pores, with attractive electrostatic potentials. The results shown for cylindrical pores are the same as in Figure 3.

The effects of pore shape are illustrated in Figure 4, using electrostatic interactions like those in Figure 3. It can be seen that for the same values of the dimensionless parameters, Φ for slit pores exceeds that for cylindrical pores, provided that $\Phi < 1$. This behavior, which is evident also for neutral, rigid molecules,[1,26] reflects the fact that slits constrain molecular position only in one dimension, whereas cylindrical pores offer constraints in two. Accordingly, wall effects tend to be weaker for slit-like pores. The weaker wall effect for slits is also responsible for the reversal of the curves when $\Phi > 1$ ($\tau\lambda_g = 2$ in Figure 4). That is, attractive interactions are experienced more strongly in cylindrical pores, so that Φ for cylindrical pores eventually exceeds that for slits, as $\tau\lambda_g$ is decreased (or $q\sigma$ made more negative).

The results for the van der Waals potential are shown in Figure 5. The hard-sphere radius was assumed to be a constant fraction of r_g, so s/λ_g is constant for each curve. Some of the curves fall below the zero-potential case ($C = 0$, $s = 0$) because the hard-sphere repulsion reduces the effective pore radius, resulting in steric exclusion of the macromolecule which cannot be overcome by the attractive portion of the potential. The values of C used in Figure 5 are representative of dispersive interactions in vacuo. In the presence of a solvent, the van der Waals interaction would be much reduced.[27] Even with values of C which tend to be too large, the short-ranged nature of the van der Waals interaction prevents any large deviation from the zero-potential case.

Discussion

The partition coefficient of a polymer is a reflection of the probability of finding the molecule within the pore, averaged over the pore cross section. One might expect from this that Φ would be insensitive to the shape of the potential function, depending mainly on the average potential in the pore. Our calculations show that this is not the case. As seen most clearly for the square-well and electrostatic results, the longer ranged the potential, the

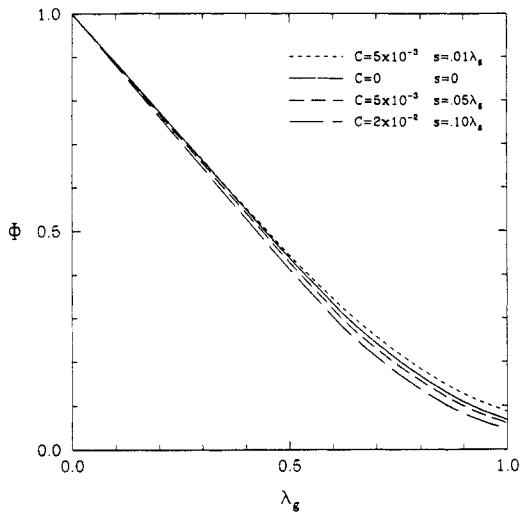

Figure 5. Partition coefficient for van der Waals potentials in a slit pore. The values of C are representative of van der Waals energy coefficients for molecules of widely varying size and polarizability.[27]

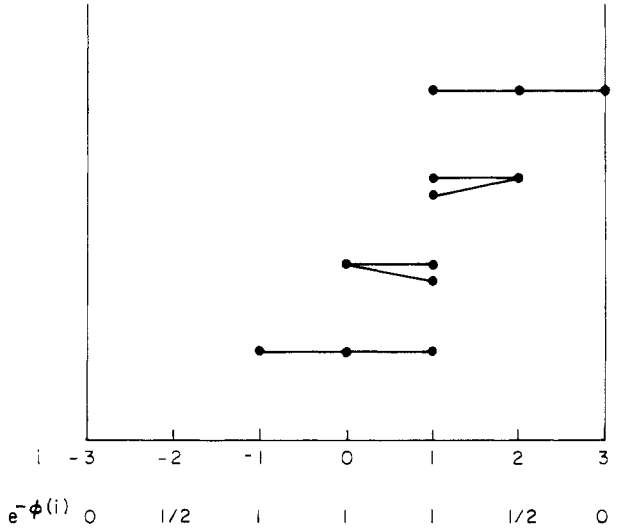

Figure 6. Representative configurations for a one-dimensional chain consisting of three mass points.

greater the effect on partitioning. The reason that Φ does not correlate very well with the average potential (or the area under the potential vs position curve) is the steric exclusion caused by the pore wall. The probability of finding a mass point of a neutral chain near the wall is already close to zero, so that short-ranged repulsions, or short ranged-attractions of moderate strength, have little effect on Φ. By contrast, longer ranged potentials are able to affect the mass point probability in regions where it is not small, thereby influencing Φ.

The possible importance of short-ranged attractions depends on the parametric conditions being examined. The present calculations assume that $\phi \ll 1$ and that $N\phi$ is finite. With these restrictions, short-ranged attractive potentials, such as those arising from highly screened electrostatic forces or from van der Waals forces, have little effect on Φ, for the reasons just mentioned. However, if ϕ is not necessarily small, and if $N\phi$ is not considered to be bounded, potentials of vanishingly short range can have large effects on Φ. This latter situation is considered elsewhere,[13] using a square-well model. Which of these assumptions is more realistic will depend on the actual physical conditions of interest.

As noted previously,[10,11,13] the diffusion equation approach provides a relatively simple method to estimate Φ for long, freely jointed chains. Because it avoids the enumeration of all chain conformations and orientations, the diffusion equation method requires much less computational effort than does a Monte Carlo calculation, provided that N is very large. An inherent limitation of the continuum, diffusion equation approach, however, is the requirement that the ratio of segment length to pore size be very small. Perhaps a more serious limitation of the calculations of Φ performed here, and those reported previously with this method,[10,11,13,16] is the neglect of intramolecular interactions. Thus, these results do not account for differences in solvent quality or, in the case of polyelectrolytes, for intramolecular electrostatic repulsion.

In principle, the effects of intramolecular interactions could be incorporated into the potential, ϕ. Suitable potentials have been formulated to describe the expansion of polymer coils due to excluded volume[17-19,28] or electrical charge.[29] These self-consistent field methods for determining ϕ assume uniform expansion of the polymer from its unperturbed, random-coiling state and therefore rely on the spherical symmetry of the probability density for isolated polymers. Because of the usual lack of spherical symmetry in a pore, the self-consistent field approach cannot be readily applied to the partitioning problem for polymers.

An alternative to modifying ϕ to account for intramolecular forces would be to adjust the "diffusion coefficient" in eq 10. In this approach, we would replace $Nl^2/6$ in eq 10 with $\alpha^2Nl^2/6$, where the molecular expansion coefficient (α) is obtained either experimentally or theoretically.[22,29] Modifying the diffusion coefficient in this manner has no rigorous basis, but the effect would be qualitatively correct in the sense that an expanded polymer coil ($\alpha > 1$) would be excluded from pores to a greater degree than would the unperturbed coil ($\alpha = 1$). Thus, including α in this way might provide a useful first approximation to the effects of intramolecular forces on Φ.

Appendix

Discrete Example. To demonstrate that the partition coefficient calculated by using eq 17 is consistent with eq 5, and to test the validity of eq 15, we present a simple example. Consider the one-dimensional pore system depicted in Figure 6. For simplicity, we limit solute chains to three mass points ($N = 3$) and restrict these mass points to discrete locations, labeled i. Each location is weighted by a Boltzmann factor, $e^{-\phi(i)}$, as defined in eq 6. The pore walls have an infinite potential, consistent with steric exclusion. In this particular example, the weighting factors for the interior points have been chosen to represent a repulsive polymer–pore interaction.

First, we calculate the partition coefficient directly from the configuration integrals in eq 5. For a chain of three mass points, there are two possible conformations, one extended and one folded. Because we have a one-dimensional system, there are also only two possible orientations: chains that are directed toward the left (relative to the first mass point) and those that are directed toward the right. Thus, there are four different combinations of conformation and orientation, as shown in Figure 6. There are five positions available to a locator point on the molecule (i.e., five interior positions), yielding a total of 20 distinct configurations.

For this discrete system, the integrals in eq 5 can be

Table I
P(i,j) for System Depicted in Figure 6

	$i = 0$	$i = 1$	$i = 2$	$i = 3$
$j = 1$	1	1	1/2	0
$j = 2$	1	3/4	1/4	0
$j = 3$	3/4	5/8	3/16	0

replaced by summations:

$$\Phi = \frac{1}{20}\sum_{i=-2}^{2}\sum_{j=1}^{2}\sum_{m=1}^{2} e^{-E_{MP}(i,\Omega_j,\Gamma_m)/kT} \tag{A1}$$

For each possible configuration, we can calculate $\exp(-E_{MP}/kT)$ by using eq 7. For example, the energy of the top configuration in Figure 6 is

$$E_{MP}/kT = \phi(1) + \phi(2) + \phi(3) \tag{A2}$$

from which we obtain

$$e^{-E_{MP}/kT} = (1)\left(\frac{1}{2}\right)(0) = 0 \tag{A3}$$

Calculating these Boltzmann factors for all 20 configurations in the pore and carrying out the summations in eq A1, we find that $\Phi = 19/40$.

We now calculate Φ by the diffusion equation or Markoff approach, using a discrete analogue of eq 6:

$$P(i,j+1) = \sum_{k=1}^{2} P[i + (-1)^k, j]\Upsilon e^{-\phi(i)} \tag{A4}$$

For this one-dimensional system, the bond probability is $\Upsilon = 1/2$; that is, in the absence of any potentials, mass point j is located with equal probability to the left or right of mass point $j + 1$. The boundary and symmetry conditions are

$$P(3,j) = 0 \tag{A5}$$

$$P(i,j) = P(-i,j) \tag{A6}$$

The initial condition (analogous to eq 15) becomes

$$P(1,1) = P(0,1) = P(-1,1) = 1 \tag{A7}$$

$$P(2,1) = P(-2,1) = 1/2 \tag{A8}$$

With these conditions, we can now evaluate $P(i,j)$ from eq A4. For example

$$P(1,2) = P(0,1)\left(\frac{1}{2}\right)e^{-\phi(1)} + P(2,1)\left(\frac{1}{2}\right)e^{-\phi(1)}$$
$$= (1)\left(\frac{1}{2}\right)(1) + \left(\frac{1}{2}\right)\left(\frac{1}{2}\right)(1) = \frac{3}{4} \tag{A9}$$

In this way, we can evaluate the solution $P(i,j)$ for all i and j, with the results summarized in Table I. (The values not shown follow from symmetry, eq A6.) Using a discrete form of eq 17 to calculate the partition coefficient, we obtain

$$\Phi = \frac{1}{5}\sum_{i=-2}^{2} P(i,3) = \frac{1}{5}\frac{19}{8} = \frac{19}{40} \tag{A10}$$

From this discrete example, we see that the two approaches to calculating Φ, which correspond to eqs 5 and 17, respectively, are equivalent. If an unweighted initial condition had been used in the Markoff calculation (replacing 1/2 by 1 in eq A8), we would have obtained $\Phi = 11/20$, which is incorrect. This supports the validity of eq 15.

Solution for Square-Well Potentials. The problem defined by eqs 11–13 and 15, with $\phi(r)$ described by the square-well potential (eq 19), can be solved by separation of variables. The solution is

$$P(r,J) = \sum_{n=1}^{\infty} A_n \exp(-\beta_n^2 J) J_0(\beta_n r/\lambda_g) \qquad 0 \le r \le 1 - d$$

$$P(r,J) = \sum_{n=1}^{\infty} C_n \exp(-\beta_n^2 J)\left[J_0(\gamma_n r) - \frac{J_0(\gamma_n) Y_0(\gamma_n r)}{Y_0(\gamma_n)}\right] \qquad 1 - d \le r \le 1 \tag{A11}$$

The eigenvalues, β_n, are described by the characteristic equation

$$0 = \frac{-\beta_n j_{11}}{\lambda_g j_{01}} G + \gamma_n (j_{12} - \chi y_{12}) \tag{A12}$$

where γ_n is related to β_n by

$$\gamma_n = \frac{1}{\lambda_g}(\beta_n^2 - W)^{1/2} \tag{A13}$$

and the constants A_n and C_n are defined as

$$A_n = \frac{C_n G}{j_{01}} \tag{A14}$$

$$C_n = \frac{(\lambda_g j_{11}/\beta_n j_{01}) DG + (1/\gamma_n)[j_{13} - Dj_{12} - F(y_{13} - Dy_{12})]}{(D^2G^2/2)[j_{11}^2/j_{01}^2 + 1] + \frac{\omega_j}{2} - H + \frac{F^2\omega_y}{2}} \tag{A15}$$

We have simplified eqs A14 and A15 by introducing the following definitions:

$$D = 1 - d \tag{A16}$$

$$F = \frac{J_0(\gamma_n)}{Y_0(\gamma_n)} \tag{A17}$$

$$G = J_0[\gamma_n(1-d)] - \frac{J_0(\gamma_n) Y_0[\gamma_n(1-d)]}{Y_0(\gamma_n)} \tag{A18}$$

$$H = 2\frac{J_0(\gamma_n)}{Y_0(\gamma_n)}\int_{1-d}^{1} J_0(\gamma_n r) Y_0(\gamma_n r) r\, dr \tag{A19}$$

$$\omega_j = J_1^2(\gamma_n) - (1-d)^2 J_1^2[\gamma_n(1-d)] + J_0^2(\gamma_n) - (1-d)^2 J_0^2[\gamma_n(1-d)] \tag{A20}$$

$$\omega_y = Y_1^2(\gamma_n) - (1-d)^2 Y_1^2[\gamma_n(1-d)] + Y_0^2(\gamma_n) - (1-d)^2 Y_0^2[\gamma_n(1-d)] \tag{A21}$$

$$j_{01} = J_0\left(\frac{\beta_n(1-d)}{\lambda_g}\right) \tag{A22}$$

$$j_{11} = J_1\left(\frac{\beta_n(1-d)}{\lambda_g}\right) \tag{A23}$$

$$j_{12} = J_1[\gamma_n(1-d)] \tag{A24}$$

$$j_{13} = J_1(\gamma_n) \tag{A25}$$

$$y_{12} = Y_1[\gamma_n(1-d)] \tag{A26}$$

$$y_{13} = Y_1(\gamma_n) \tag{A27}$$

The integral in eq A19 was evaluated numerically. In eqs A11–A27, J_0 and J_1 are Bessel functions of the first kind of order zero and one, respectively; Y_0 and Y_1 are Bessel functions of the second kind of order zero and one.

From eq A13, we see that, depending on the magnitude and sign of W, β_n and γ_n can be either imaginary or real. In writing eqs A11–A27, we have assumed that both β_n and γ_n are real. The three possible solutions in which either β_n alone is imaginary, γ_n alone is imaginary, or both β_n and γ_n are imaginary can be obtained from eqs A11–A27 by making the substitutions $\beta_n = i\mu_n$ and $\gamma_n = i\nu_n$. The resulting eigenfunctions are modified Bessel functions of the real arguments μ_n or ν_n.

The solution for the square-well potential in the slit pore is similar to that in the cylindrical pore. In Cartesian coordinates, the eigenfunctions are sines, cosines, hyperbolic sines, or hyperbolic cosines, depending on whether the quantities β_n and γ_n are real or imaginary.

The Critical Point for Adsorption. Wiegel[21] determined the critical energy for adsorption of a linear polyelectrolyte on a charged, flat surface. His approach was to solve eq 10 for that geometry, which could be done analytically, and to examine the signs of the resulting eigenvalues. The energy at which eigenvalues began to change sign was interpreted as defining a phase transition between unadsorbed and adsorbed polymer. We consider here the nature of the analogous critical conditions for polymers in pores.

To determine numerically the existence of a critical point, we examined the stability of the solution to eq 10 for pores, as has been done for analogous dynamic systems.[30,31] We first discretized the spatial part of eq 10:

$$\partial \bar{P}/\partial J = \mathbf{M}\bar{P} \tag{A28}$$

where the matrix $\mathbf{M}$ includes the discretized form of both ∇^2 and $N\phi$. We then assumed a solution to eq A28 of the form

$$\bar{P} = \bar{P}^* + \bar{z}\exp(\eta J) \tag{A29}$$

where $\bar{P}^*$ is the "steady-state" solution and $\bar{z}\exp(\eta J)$ is the "transient" (J-dependent) solution. The stability of the solution to eq A28 depends on the eigenvalues η of $\mathbf{M}$, which satisfy the relation

$$\det(\mathbf{M} - \eta\mathbf{I}) = 0 \tag{A30}$$

In eq A30, $\mathbf{I}$ is the identity matrix. When all eigenvalues, $\eta_1, \eta_2, ..., \eta_n$, are negative, $\bar{P}$ evolves to the "steady-state" solution $\bar{P}^*$; when any eigenvalue is positive, the system is unstable, which is analogous to the case of adsorption in Wiegel's study.

The problem of finding the critical point is then reduced to one of determining the sign of the eigenvalues in eq A30. By use of a central difference operator to discretize eq 10, the matrix $(\mathbf{M} - \eta\mathbf{I})$ is

$$(\mathbf{M} - \eta\mathbf{I}) = \begin{bmatrix} -(2\gamma+N\phi_1+\eta) & 2\gamma & & & \\ \frac{1}{2}\gamma & -(2\gamma+N\phi_2+\eta) & \frac{3}{2}\gamma & & \\ & \ddots & \ddots & & \\ & \gamma\left[1-\frac{1}{2(i-1)}\right] & -(2\gamma+N\phi_i+\eta) & \gamma\left[1+\frac{1}{2(i-1)}\right] & \\ & & \ddots & \ddots & \\ & & & \gamma\left[1-\frac{1}{2(n-1)}\right] & -(2\gamma+N\phi_n+\eta) \end{bmatrix} \tag{A31}$$

where ϕ_i is the discretized form of $\phi(r)$, $\gamma = \lambda_g^2/h^2$, and h is the step size for integration in the r-direction. The matrix $(\mathbf{M} - \eta\mathbf{I})$ is a tridiagonal matrix of the form

$$(\mathbf{M} - \eta\mathbf{I}) = \begin{bmatrix} a_1 & c_1 & & & \\ b_2 & a_2 & c_2 & & \\ & \ddots & \ddots & \ddots & \\ & & b_{n-1} & a_{n-1} & c_{n-1} \\ & & & b_n & a_n \end{bmatrix} \tag{A32}$$

We define a sequence of polynomials

$$\begin{aligned} p_0(\eta) &= 1 \\ p_1(\eta) &= a_1(\eta)p_0(\eta) \\ &\vdots \\ p_i(\eta) &= a_i(\eta)p_{i-1}(\eta) - c_{i-1}b_i p_{i-2}(\eta) \\ p_n(\eta) &= a_n(\eta)p_{n-1}(\eta) - c_{n-1}b_n p_{n-2}(\eta) \end{aligned} \tag{A33}$$

where η is any real number. The polynomials defined in eq A33 form a Sturmian sequence,[32,33] so the number of sign changes between successive terms in the sequence $p_0(\eta), p_1(\eta), ..., p_n(\eta)$ equals the number of roots which are less than η. Therefore, by evaluating the polynomials at $\eta = 0$, we can determine the number of negative roots in eq A30. By varying the parameters ϕ_i, we can then determine the critical energy for adsorption. In the case of electrostatic particle–pore interactions, we varied ϕ by varying the product $q\sigma$. We refer to the largest value of $q\sigma$ for which all eigenvalues are negative as $(q\sigma)_{crit}$. We calculated $(q\sigma)_{crit}$ for both cylindrical and slit-shaped pores.

For slit pores with $\lambda_g = 0.2$, our values for $(q\sigma)_{crit}$ were virtually identical with those obtained from Wiegel's formula (within 0.2% for $2 \leq \tau\lambda_g \leq 5$). This is not surprising, in that Wiegel's problem is equivalent to that for a slit pore in which the wall spacing greatly exceeds the dimensions of the macromolecule (i.e., $\lambda_g \ll 1$). For all values of λ_g examined ($0.2 \leq \lambda_g \leq 2.0$), in both slits and cylindrical pores, $(q\sigma)_{crit}$ was within 20% of the value of $q\sigma$ required to yield $\Phi = 1$. We conclude that for pores the analogue to Wiegel's critical energy for adsorption is the energy at which $\Phi \simeq 1$. As already noted, this is the energy at which the entropic and enthalpic effects on partitioning just offset one another.

Pouchlý[16] has also examined the stability of the solution to the diffusion equation for polymers in pores but for different potentials and boundary conditions than we have considered. Pouchlý's problem permitted the analytical determination of eigenvalues, as did the cases considered by Wiegel[21] and others.[17,19,20] Similarly, in our analytical solution for the square-well potential, a critical condition is defined by the emergence of imaginary values of β_n in eq A11. Finally, a critical energy for adsorption of polymers in pores was also identified by Davidson and Deen.[13]

Acknowledgment. This work was supported by a grant from the National Institutes of Health, DK 20368.

References and Notes

(1) Giddings, J. C.; Kucera, E.; Russell, C. P.; Myers, N. M. *J. Phys. Chem.* **1968**, *72*, 4397.
(2) Ogston, A. G. *Trans. Faraday Soc.* **1958**, *54*, 1754.
(3) Limbach, K. W.; Nitsche, J. M.; Wei, J. *AIChE J.* **1989**, *35*, 42.
(4) Smith, F. G.; Deen, W. M. *J. Colloid Interface Sci.* **1983**, *91*, 571.
(5) Post, A. J.; Glandt, E. D. *J. Colloid Interface Sci.* **1985**, *108*, 31.

(6) Glandt, E. D. *J. Colloid Interface Sci.* **1980**, *77*, 512.
(7) Anderson, J. L.; Brannon, J. H. *J. Polym. Sci., Polym. Phys. Ed.* **1981**, *19*, 405.
(8) Mitchell, B. D.; Deen, W. M. *J. Membr. Sci.* **1984**, *19*, 75.
(9) Fanti, L. A.; Glandt, E. D. *J. Colloid Interface Sci.* **1990**, *135*, 385, 396.
(10) Casassa, E. F. *J. Polym. Sci., Polym. Lett. Ed.* **1967**, *5*, 773.
(11) Casassa, E. F.; Tagami, Y. *Macromolecules* **1969**, *2*, 14.
(12) Davidson, M. G.; Suter, U. W.; Deen, W. M. *Macromolecules* **1987**, *20*, 1141.
(13) Davidson, M. G.; Deen, W. M. *J. Polym. Sci., Polym. Phys. Ed.* In press.
(14) Zhulina, E. B.; Gorbunov, A. A.; Birshtein, T. M.; Skvortsov, A. M. *Biopolymers* **1982**, *21*, 1021.
(15) Gorbunov, A. A.; Zhulina, E. B.; Skvortsov, A. M. *Polymer* **1982**, *23*, 1133.
(16) Pouchlý, J. *J. Chem. Phys.* **1970**, *52*, 2567.
(17) de Gennes, P.-G. *Rep. Prog. Phys.* **1969**, *32*, 187.
(18) Yamakawa, H. *Modern Theory of Polymer Solutions*; Harper and Row: New York, 1971; pp 110–118.
(19) Jones, I. S.; Richmond, P. *J. Chem. Soc., Faraday Trans. 2* **1977**, *73*, 1062.
(20) Lepine, Y.; Caille, A. *Can. J. Phys.* **1978**, *56*, 403.
(21) Wiegel, F. W. *J. Phys. A* **1977**, *10*, 299.
(22) Flory, P. J. *Principles of Polymer Chemistry*; Cornell University Press: Ithaca, NY, 1953.
(23) de Gennes, P.-G. *Scaling Concepts in Polymer Physics*; Cornell University Press: Ithaca, NY, 1979; pp 246–248.
(24) DiMarzio, E. A. *J. Chem. Phys.* **1965**, *42*, 2101.
(25) Press, W. H.; Flannery, B. P.; Teukolsky, S. A.; Vetterling, W. T. *Numerical Recipes*; Cambridge University Press: Cambridge, 1986; pp 637–638.
(26) Deen, W. M. *AIChE J.* **1987**, *33*, 1409.
(27) Israelachvili, J. N. *Intermolecular and Surface Forces*; Academic Press: London, 1985.
(28) Reiss, H. *J. Chem. Phys.* **1967**, *47*, 186.
(29) Bailey, J. M. *Macromolecules* **1977**, *10*, 725.
(30) Derby, J. J.; Atherton, L. J.; Thomas, P. J.; Brown, R. A. *J. Scientific Comput.* **1987**, *2*, 297.
(31) Glass, L. In *Modern Theoretical Chemistry. Vol. 6. Statistical Mechanics, Part B. Time Dependent Processes*; Berne, B. J., Ed.; Plenum: New York, 1977, pp 29–32.
(32) Acton, F. S. *Numerical Methods That Work*; Harper and Row: New York, 1970; pp 331–334.
(33) Amundson, N. R. *Mathematical Methods in Chemical Engineering*; Prentice-Hall: Englewood Cliffs, NJ, 1974; pp 143–147.

Mutual Diffusion of Block Polymer and Homopolymer. Visualization Using Microdomain as a Probe

Satoshi Koizumi, Hirokazu Hasegawa, and Takeji Hashimoto*

Department of Polymer Chemistry, Faculty of Engineering, Kyoto University, Kyoto 606, Japan

Received October 2, 1989; Revised Manuscript Received November 30, 1989

ABSTRACT: Poly(styrene-*b*-isoprene) block polymer (SI), which forms spherical microdomains of polyisoprene (PI) block chains in the matrix of polystyrene (PS) block chains, and a mixture of SI with homopolystyrene (HS), which forms spherical microdomains of PI in the matrix of HS and PS block chains, were welded with HS with a molecular weight smaller than that of PS. The welded samples were annealed at 150 °C as a function of time, and a spatial distribution of PI spherical microdomains across the welded interface $\phi(x)$ (x being a distance normal to the interface) was observed under a transmission electron microscope in order to investigate mutual diffusion of HS molecules and PI spherical microdomains with PS chains emanating from them. The mutual diffusion coefficient, D, was found to increase with increasing the volume fraction of HS (Ψ_{HS}) initially solubilized into the microdomain space and with decreasing the molecular weight of HS (M_{HS}). D was found to be controlled primarily by the free energy barrier $\delta\Delta F^*(\Psi_{HS}, M_{HS})$ required for solubilization of HS into the matrix of the microdomain systems in the mutual diffusion process. The free energy barrier for the mutual diffusion process, $\delta\Delta F^*$, in turn, is associated with a loss of conformational entropy of the HS and PS block chains in the solubilization process, which involves breakup of the molecular interactions of PS block chains. More precisely, we found that the diffusion process does not generally obey a simple Fickian diffusion; the concentration profile $\phi(x)$ is asymmetric, and D depends on the local concentration of HS ($\phi_{HS}(x)$), that is, the larger the $\phi_{HS}(x)$, the larger the value $D(x)$, and hence on space x.

I. Introduction

Mutual diffusion of polymers in bulk is an interesting research topic in polymer physics.[1-4] Here we propose visual observations of the mutual diffusion process of a unique polymer system. We study a mutual diffusion of a block polymer and a homopolymer, which are welded together at their fractured surfaces.

The block polymer system we used in this study is poly(styrene-*b*-isoprene) (SI) which forms spherical microdomains of polyisoprene block chains (PI) in the matrix of polystyrene block chains (PS) as shown schematically in Figure 1a. We used also a mixture of SI and homopolystyrene (HS), which forms PI spherical microdomains in the matrix of PS and HS as shown schematically in Figure 1b. HS was more or less uniformly solubilized into PS matrix formed by segregation of the block polymer.

SI block polymer in bulk or the bulk of the block polymer containing HS is welded with bulk HS at their surfaces, as shown schematically in Figure 2. The welded samples are then annealed at temperatures above glass transition temperatures of PS and HS to allow the mutual diffusion of HS chains and PI spheres across the welded interface. PI spheres have many PS chains emanating from them ("PS coronas"). The mutual diffusion will cause a change of spatial distribution of PI spheres across the interface as schematically sketched in parts a and b of

0024-9297/90/2223-2955$02.50/0 © 1990 American Chemical Society